




A parametric study and characterization of additively manufactured continuous carbon fiber reinforced composites for high-speed 3D printing

John M. Pappas¹ · Aditya R. Thakur¹ · Ming C. Leu¹ · Xiangyang Dong¹ 

Received: 2 November 2020 / Accepted: 28 January 2021 / Published online: 18 February 2021
© The Author(s), under exclusive licence to Springer-Verlag London Ltd. part of Springer Nature 2021

Abstract

High-speed 3D printing has recently gained much interest due to its potentials in improving efficiency of fabricating complex geometry components and applications in large-scale additive manufacturing (AM). In this study, a parametric study is performed experimentally to investigate factors affecting high-speed 3D printing of continuous carbon fiber reinforced composites (CFRCs), including material deposition rate, print (nozzle traverse) speed, and nozzle tilt angle based on a novel multi-axis AM approach. The method uses thermoplastic pellets and continuous carbon fiber tows as feedstock materials. The obtained sample quality and mechanical properties are investigated with respect to deposition rate, print speed, and nozzle tilt angle. The fiber impregnation quality is examined through microstructure analysis and correlated with the process conditions and mechanical properties. Increasing deposition rate and tilt angle both improve fiber impregnation quality, enabling implementation of higher print speed and yielding improved mechanical properties. This, combined with demonstrations of printed complex geometry components, shows the great potentials of the proposed method for AM of continuous CFRCs at high speeds. The results of this study also provide further guidance on design and manufacturing of large-volume, high-strength CFRCs through 3D printing.

Keywords Additive manufacturing · Carbon fiber reinforced composite · Continuous fiber reinforcement · High-speed 3D printing

1 Introduction

Carbon fiber reinforced composites (CFRCs) have gained increasing interests in additive manufacturing (AM) for applications in automotive, civil, and aerospace industries as lightweight, high-strength materials [1, 2]. AM enables enormous flexibility in CFRC product design while significantly reducing manufacturing costs and simplifying fabrication processes. Recent studies have investigated CFRC samples fabricated with varying carbon fiber length [3–8] in carbon fiber reinforcement using the fused filament fabrication (FFF) method [2, 9–11].

Among the various FFF-based studies, AM of high-strength CFRC was achieved via impregnating continuous carbon fibers for reinforcement [11, 12]. However, the manufacturing costs involved are typically very high, like commercial 3D printers including Markforged, mainly attributed to the requirement of using specialized fiber reinforced filaments as feedstock. This inadvertently reduces customizability in design of fiber reinforced composites [13, 14]. In addition, the low throughput (typically at a deposition rate of about 0.46 g/min) makes it practically infeasible to fabricate large structures [11, 15]. The filament diameter, geometry, and feed speed need to be carefully controlled in order to ensure high printing quality, which substantially increases the manufacturing costs resulting in the price of thermoplastic composite filament with seemingly low-cost thermoplastics to as high as \$100/kg [16]. Other promising manufacturing methods including automated thermoplastic tape laying (ATL) and automated fiber placement (AFP) also allow continuous fiber reinforcement [17]. However, capital expenditures for such computer-driven, automated equipment can be significant with additional requirements for molds [18].

John M. Pappas and Aditya R. Thakur contributed equally to this work.

✉ Xiangyang Dong
dongxi@mst.edu

¹ Mechanical and Aerospace Engineering, Missouri University of Science and Technology, Rolla, MO 65409, USA

The increasing demand for customizable, large-scale additively fabricated structures necessitates the development of corresponding AM techniques with high print speeds. To address this need, large-scale additive manufacturing has been developed by directly using thermoplastic pellets as feedstock (e.g., Big Area Additive Manufacturing (BAAM) [19], Gigabot X [20], and CEAD Composite Additive Manufacturing [21]). A high deposition rate ($> 200\times$) can be achieved through pellet-based extrusion processes compared to conventional filament-based extrusion processes (i.e., FFF method). Meanwhile, the manufacturing costs have been dramatically reduced ($\sim 100\times$) with a wider variety of thermoplastics available as the feedstock material, even including recycled thermoplastics [20].

In fabrication of CFRC components, a majority of existing studies utilized short fiber-reinforced pellets as feedstock. Compared to short fiber reinforcement, directly using continuous fibers and thermoplastic pellets as feedstock can potentially achieve higher mechanical strength. An in situ extrusion method [22, 23] was implemented to 3D printing of continuous CFRCs. However, the achieved material deposition rate was still relatively low, comparable to the conventional FFF method. For thermoplastics reinforced with continuous carbon fibers, one major factor governing the CFRC strength is fiber-matrix interface [9, 11]. The obtained mechanical properties are mainly affected by the wetting condition of carbon fibers by the thermoplastic melt during the AM process, which is related to the processing parameters including printing temperature, layer thickness, and hatch spacing [11]. However, only the effect of relative low deposition rate (e.g., 0.46 g/min) on fiber-matrix interface of continuous CFRCs was investigated. To our best knowledge, very few studies have been performed to explore the effect of relatively higher material deposition rate on AM of continuous CFRCs, which is particularly necessary for high-speed 3D printing.

Multi-axis AM techniques have been studied using multi-axis CNC systems, robotic or rotational printing platforms [24]. However, this functionality has only been explored to either enable defect-free fabrication of conformal features on curved surfaces [25], prevent stair-step effect, manufacture orthogonal preforms [26], or support-free or overhanging lattice structures [27]. Non-planer extrusion-based AM methods have also been studied to enhance the mechanical properties of the 3D printed structures by multi-plane layering or moderating laydown paths to align with the direction of stress within the structures [28]. This has been further enhanced by incorporation of continuous fiber reinforced filaments [29, 30], achieving improved stiffness and higher peak load on the 3D printed structures by reducing intra- and inter-layer failure due to anisotropic distribution of loads along material deposition paths. However, to the best of our knowledge, very few studies have been performed to

study multi-axis AM processes on the obtained microstructure and mechanical properties of continuous CFRCs themselves.

In this study, a multi-axis AM technique using a pellet-based extrusion process was investigated to fabricate continuous CFRC samples. Continuous carbon fibers and thermoplastic pellets were directly used as feedstock. Several factors affecting high-speed 3D printing were explicitly studied, including material deposition rate, print (nozzle traverse) speed, and nozzle tilt angle for the proposed multi-axis AM technique. The effects of these parameters on mechanical properties and microstructure of obtained continuous CFRC samples were investigated. The fiber-matrix interface was further characterized and correlated with obtained mechanical properties under different printing conditions. Specifically, a deposition rate up to 13.3 g/min was examined in this study. Although the multi-axis 3D printing process was demonstrated before for continuous CFRCs [23], the effect of nozzle tilt angle on obtained CFRC microstructure and its relationship to mechanical properties has only been limitedly studied, which was found to have significant benefits in facilitating high-speed 3D printing in this study.

2 Experimental procedure

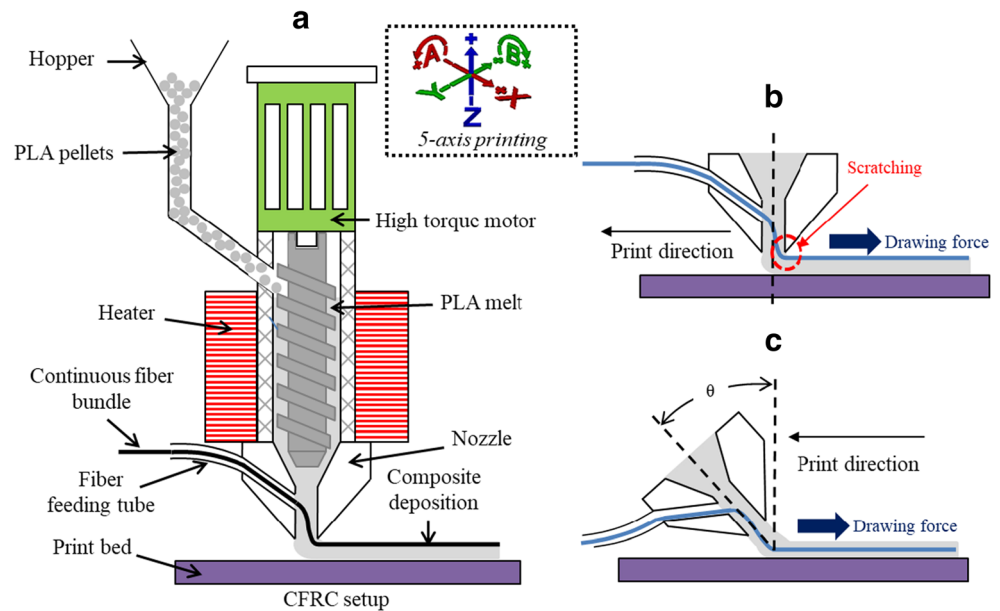
2.1 Material preparation

Commercially available transparent polylactic acid (PLA) pellets (4043D by Filabot) were used as feedstock material for thermoplastic matrix to facilitate the characterization of printed CFRC samples. 3 K (3000 filaments in a bundle) continuous carbon fibers (by AS4C by Hexcel) were selected as the reinforcement material for the CFRC samples. The PLA pellets were first dried in a vacuum oven at 85 °C for at least 4 h to eliminate moisture before printing. The presence of moisture could hydrolyze PLA in the melt phase, which would reduce its molecular weight and promote bubble formation during extrusion, lowering mechanical properties of the printed samples. The carbon fiber tows were dried in the vacuum oven at 120 °C for at least 4 h to remove the moisture and minimize fiber clumping during extrusion. Clumping can be detrimental to the deposition quality and CFRC mechanical properties and is aggravated by the presence of moisture [31].

2.2 Experimental setup

The experimental setup is shown in Fig. 1a, including a single-screw extruder (MDPH2), a multi-axis machine (Galaxy G by Automated Precision Inc.), and an acrylic print bed. During printing process, PLA pellets were fed through the extruder hopper and melted by the heater before being extruded out through the nozzle. Meanwhile, a continuous carbon fiber

Fig. 1 **a** shows the experimental setup used for AM of continuous CFRC samples. **b** and **c** demonstrate the multi-axis printing process with a tilt angle (θ) to minimize scratching



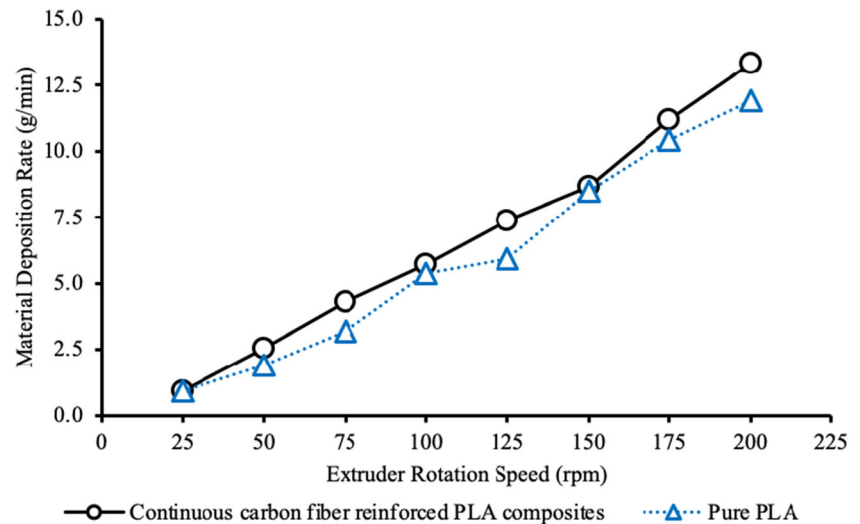
bundle was impregnated while passing through the extrusion nozzle [2] and then coextruded with the thermoplastics melt for deposition on the print bed layer-by-layer. The movement of the extruder was controlled by the multi-axis machine. Compared to previous studies where the extruder was commonly mounted vertically during 3D printing (Fig. 1b), a multi-axis 3D printing process is implemented in this study. The nozzle tilt angle (θ) is maintained constant as shown in Fig. 1c, while the nozzle movement follows the print toolpath in three-dimensional space. The nozzle tilting is hypothesized to minimize the potential scratching of continuous carbon fibers and fiber breakage caused by extrusion nozzle due to drawing forces during the 3D printing process, thereby enabling the implementation of a high print speed. In this study, the tilt angle was varied between 0° and 35° to study its effect on printing process and mechanical properties.

The implementation of the single-screw extruder can help achieve a high material deposition rate, which is typically desired for high-speed 3D printing. The extrusion screw was driven by a high torque motor. The inner diameter of the coextrusion nozzle is closely related to the printing resolution as well as the material deposition rate. A nozzle of 4-mm diameter was selected in this study to achieve printing parts with decent resolution yet still being able to achieve a relatively high material deposition rate. With a constant melting temperature of 190°C in this study, the obtained material deposition rate is determined by the rotation speed of extrusion screw [11, 32]. Thus, the material deposition rates were first calibrated: the materials were extruded for a fixed, short period of time with the rotation speed varying between 25 and 200 rpm; the weight of the deposited material was measured to calculate the material deposition rate (g/min). Figure 2

shows the measured material deposition rate with respect to the extrusion rotation speed (rpm) for both pure PLA and continuous CFRCs using the current experimental setup.

An approximately linear trend between the material deposition rate and the extruder rotation speed was observed for both pure PLA and continuous CFRCs. As expected, due to the introduction of carbon fibers, the deposition rate of continuous CFRCs was slightly higher than that of pure PLA. At the extruder rotation speed of 200 rpm, a maximum deposition rate of 13.3 g/min was achieved in this study, over 28 times the deposition rate (e.g., 0.46 g/min [11, 15]) used by a typical FFF process. It should be noted that the material deposition rate can also be scaled up (e.g. 833.3 g/min [16]) with a further optimized setup. In this study, we focused on a relatively higher material deposition rate domain compared to previous studies [11, 15], in order to examine its effects on obtained continuous CFRC samples for potential applications on high-speed 3D printing. Thus, the material deposition rate was varied from 0.9 to 13.3 g/min to study its effect on printed continuous CFRC samples. It is also worth noting that while this study investigated the fiber-matrix interface and its relationship with mechanical properties of CFRC samples, the bonding between deposition layers also plays a critical factor affecting the mechanical strength of the printed composites [11, 33] as further affected by deposition layer thickness. A layer thickness of 1.5 mm was selected in this study, where no delamination between layers was found during mechanical testing of all printed CFRC samples. With the selected 3D printing conditions, a maximum carbon fiber content of 10.5 vol.% was obtained for the printed continuous CFRC samples.

Fig. 2 Material deposition rates of pure PLA and continuous CFRCs with varying extrusion rotation speeds at the melting temperature of 190 °C

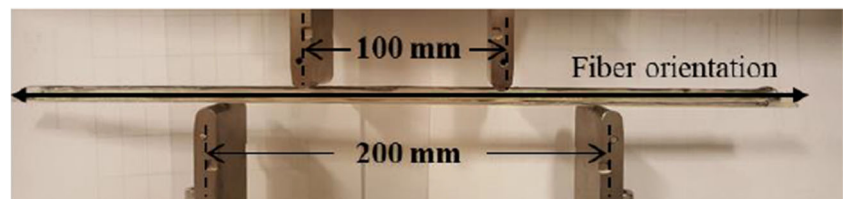


2.3 Mechanical testing and microstructure characterization

Mechanical tests were carried out following ASTM standard D7264/D7264M-15. Flexural strength and modulus of the additively fabricated CFRC samples are measured through four-point bending tests in Fig. 3 as they are closely related to fiber-matrix interfacial bonding [34]. Rectangular test bars with a length of 400 mm were prepared by 3D printing thin-wall structures with 7 deposition layers. Flexural strength and modulus are determined using an Instron 5881 machine with a support span of 40 mm and a load span of 20 mm as shown in Fig. 3. Three samples under each printing condition were tested at a cross-head speed of 1 mm/min.

To correlate the measured mechanical strength with the printing conditions, the fracture surfaces and polished cross sections [35–37] of the printed CFRC samples were examined to analyze microstructure and fiber-matrix interface. The CFRC samples were sectioned using a slow-speed diamond saw and polished using diamond polishing discs with up to 3 μm in grit size. The polished cross sections of the CFRC samples were then examined under a Hirox Digital KH-8700 Optical Microscope and a Quanta 600F Environmental Scanning Electron Microscope to study the fiber-matrix interface. FIJI image analysis software was used to binarize and threshold the microscopic images to determine the void area fraction using the built-in particle analysis function [38].

Fig. 3 Four-point bending test setup and demonstration of fiber orientation



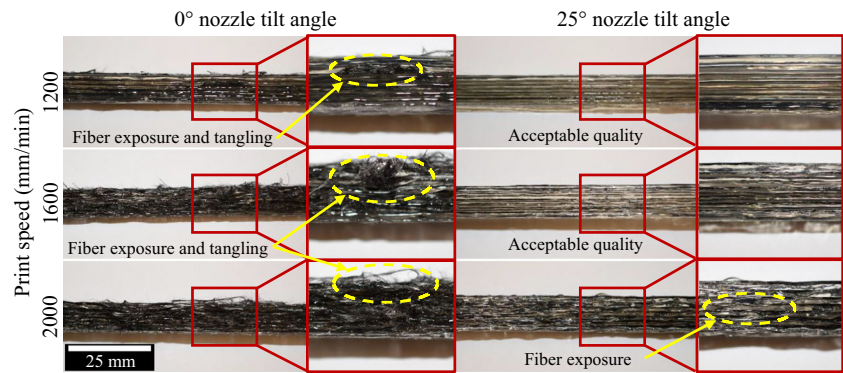
3 Results and discussion

3.1 Printability

The feasibility of the proposed AM method for preparing continuous CFRC samples was first investigated through examining the printability window based on selected printing conditions, including material deposition rate, print speed, and nozzle tilt angle. The print speed in this study denotes the traverse speed of extrusion nozzle. At a fixed material deposition rate, it is critical to determine the range of print speeds for feasible printing quality [11]. With improper print speeds, lack of extruded matrix material would cause fiber exposure. The exposed fibers would be more easily damaged and tangled together, worsening printing resolution and mechanical properties. This is particularly critical for high-speed 3D printing, where a high print speed and a high material deposition rate are preferred. Feasibility tests are thus first carried out through printing straight long bar samples in Fig. 4. The acceptable print quality was defined for those CFRC samples with no visible fiber exposure or tangling, yielding good print resolution.

As shown in Fig. 4, at the material deposition rate of 5.7 g/min, increasing print speed would increase fiber exposure due to gradually insufficient amount of extruded matrix materials (i.e., lack of materials). During the printing process, the continuous carbon fiber bundle was under tension due to the

Fig. 4 Comparison of the continuous CFRC samples printed at nozzle tilt angles of 0° and 25° and print speeds of 1200, 1600, and 2000 mm/min. A constant material deposition rate of 5.7 g/min was used for all samples



drawing force of deposited composite materials. With the extruder mounted vertically ($\theta=0^\circ$ in Fig. 1b), the exposed carbon fiber bundle would be more easily scratched by the extrusion nozzle tip under an increased drawing force at a higher print speed. Part of carbon fibers within the bundle would then be tangled together, forming fiber clumps and hindering smooth flow of melted matrix material. These fiber clumps result in an irregular print geometry throughout the deposited structures shown in Fig. 4.

While increasing the material deposition rate would compensate the lack of materials at a higher print speed, increasing the nozzle tilt angle (Fig. 1c) is presumed to enable a smoother flow of extrudate during printing. As shown in Fig. 4, a higher nozzle tilt angle (25°) lowers the fiber exposure and eliminates fiber tangling due to scratching. This will not only achieve improved carbon fiber reinforcement, making the fiber better enveloped within the matrix material, but also allow the implementation of much higher print speeds. It is worth noting that the exposed fiber may be broken due to scratching, lowering the mechanical properties, which were also examined in detailed microstructural analysis in Section 3.3.3 for varying nozzle tilt angles.

A process map is plotted in Fig. 5 based on the quality of printed samples for varying print speeds and material deposition rates. Two different nozzle tilt angles were included for comparison, i.e., 0° and 25° . Initial testing of samples printed with a material deposition rate of 5.7 g/min, print speed of 800 mm/min, and nozzle tilt angles ranging from 0° to 35° revealed that a nozzle tilt angle of 25° minimized fiber breakage due to scratching and maximized mechanical properties. Hence, the process map was also determined for a nozzle tilt angle of 25° . For a given material deposition rate, fiber exposure and tangling will occur if the print speed is too high. Thus, a printability window, denoted by dashed (0°) and dash-dotted lines (25°), is obtained as shown in Fig. 5, where all processing conditions within the printability window yielded acceptable print quality. As expected, as the material deposition rate increased, a higher maximum print speed was obtained since the additional extruded matrix material compensated for the lack of material that led to fiber exposure and tangling.

The implementation of a higher nozzle tilt angle dramatically increased the size of the printability window, specifically increasing the maximum print speed for acceptable print quality under the same material deposition rates. A higher maximum print speed was consistently obtained when the extruder was tilted from 0° to 25° in printing of CFRC samples at a material deposition rate higher than 0.9 g/min. Within the range of selected material deposition rates, the print speed cannot go above 1400 mm/min with the nozzle tilt angle of 0° due to severe fiber tangling. In contrast, a print of speed of up to 3400 mm/min was achieved at a deposition rate of 13.3 g/min with the nozzle tilt angle of 25° . It is worth noting that while it was hypothesized that including a positive nozzle tilt angle may reduce the fiber scratching effect and thus allow for acceptable deposition quality at print speeds higher than what was possible when the extruder nozzle was oriented at 0° , a direct comparison of printability windows in Fig. 5 shows a significant improvement (i.e., nearly 2.5-fold), which is achieved in the maximum print speed by tilting the nozzle via the proposed multi-axis AM method. This well demonstrated its great potentials for high-speed 3D printing of continuous CFRCs, reducing component build times and increasing printing efficiency, thus worth further implementation of the multi-axis AM method for fabrication of large-scale CFRC components.

3.2 Mechanical properties

3.2.1 Effect of material deposition rate

The mechanical properties of the printed CFRC samples using the printing conditions within the printability window in Fig. 5 are further studied. It is worth noting that the previous studies typically used FFF processes, where a relatively low deposition rate domain was studied, e.g., varying between 0.17 and 0.46 g/min [11]. No obvious effect on mechanical properties was reported. To explore the effect of deposition rate at a higher rate domain, as desired by high-speed 3D printing, the mechanical properties of the continuous CFRC samples printed with material deposition rates of 4.3 g/min up to 13.3

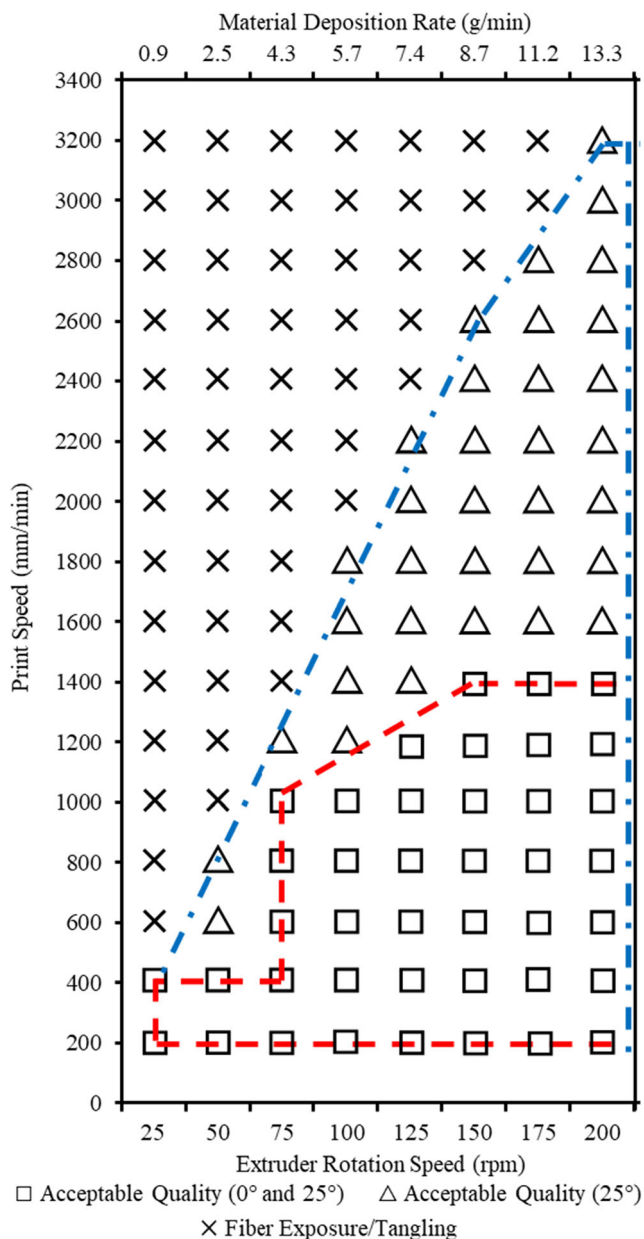


Fig. 5 Process map for continuous CFRC samples at various print speeds and deposition rates. Two printability windows are marked to show proper conditions yielding acceptable print quality. The dashed lines denote the range of acceptable print quality with a 0° nozzle tilt angle. The dash-dotted lines represent the range of acceptable print quality achieved by a 25° nozzle tilt angle

g/min, corresponding to extruder rotation speeds of 75 to 200 rpm at 25-rpm intervals, are first measured and compared in Fig. 6. The printability window was used to guide parameter selection for this study, and a print speed of 800 mm/min selected since it corresponded to a wide range of material deposition rates that resulted in acceptable deposition quality, minimal fiber breakage, and relatively high-speed printing. For comparison, the PLA samples without fiber reinforcement were also tested and included. As expected, for pure PLA samples, increasing deposition rates had no obvious effect

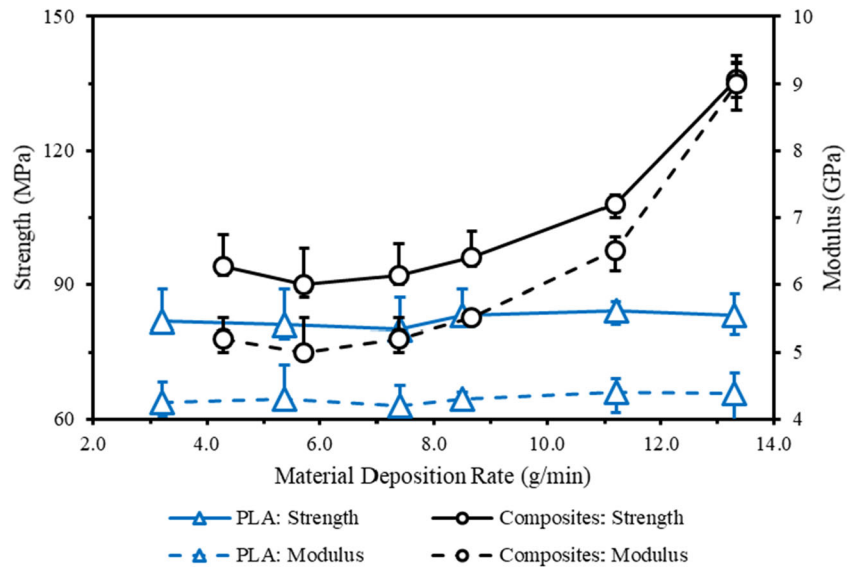
on the obtained flexural strength and modulus. In contrast, a general trend observed for the continuous CFRC samples was that with an increase in material deposition rate, a higher flexural strength and a higher flexural modulus were obtained. At a deposition rate of 13.3 g/min, the measured values of flexural strength and modulus dramatically increased to an average of 140 MPa and 8.5 GPa, respectively. Compared to those measured at 4.3 g/min, an improvement of 44.7% and 73.1% in flexural strength and modulus, respectively, was achieved. The increase in mechanical properties in Fig. 6 is believed to be due to better wetting conditions between the PLA matrix and carbon fibers achieved at higher material deposition rates, which was further examined by microstructure characterization in Section 3.3.1. The observed trend indicated that increasing the material deposition rate not only achieved higher printing efficiency as desired by high-speed 3D printing process but also achieved better mechanical properties for the printed CFRC parts. Thus, it will be worth further exploring the effects of even higher material deposition rates achieved through pellet-based extrusion processes.

It is also worth noting that the relatively moderate improvement in mechanical properties was attributed to a relatively low carbon fiber volume fraction (a maximum of 10.5 vol.%) achieved with 3 K carbon fibers used in this study. Our preliminary studies have shown that a higher fiber volume fraction could be achieved if a larger carbon fiber bundle size is used. For example, increasing from 3 K fibers to 12 K fibers (12,000 filaments in a bundle), a maximum 41.9 vol.% in fiber volume fraction could be obtained using the same experimental setup. However, the use of larger carbon fiber bundle size also poses additional challenges (e.g., easier fiber exposure and tangling) in the 3D printing process of continuous CFRC samples and will be further investigated in our future studies.

3.2.2 Effect of print speed

A higher print (nozzle traverse) speed is also desired for a high-speed 3D printing process. The effect of print speed within the printability windows found in Fig. 5 is thus investigated. It should be noted that all the tested CFRC samples exhibited acceptable print quality with no fiber tangling/exposure. Parameter selection was based on the obtained printability window with print speeds varying from 400 to 1000 mm/min at 200 mm/min intervals. The mechanical properties of CFRC samples printed at a constant deposition rate of 5.7 g/min and a nozzle tilt angle of 0° are measured and compared in Fig. 7. The material deposition rate was chosen since it provided several viable print speeds that resulted in acceptable deposition quality while maintaining a relatively higher fiber volume fraction. With no fiber reinforcement for the PLA samples, changing the printing speed only led to small variations in the obtained flexural strength and modulus. In

Fig. 6 Flexural strength and modulus measured through four-point bending tests for continuous CFRC samples at a print speed of 800 mm/min and a nozzle tilt angle of 0° with varying material deposition rates. PLA samples were also tested and included for comparison



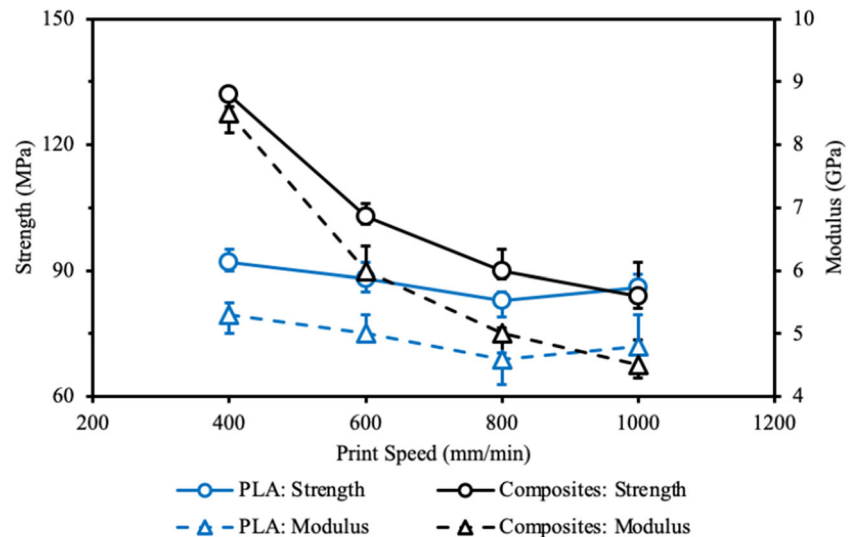
contrast, for the CFRC samples, both flexural strength and modulus consistently and significantly decreased as the print speed increased. The results indicated that high-speed 3D printing cannot simply be achieved by increasing the print speed without sacrificing obtained mechanical properties. The decreasing CFRC flexural strength and modulus with respect to increasing print speed is believed to be affected by residual voids within the obtained CFRC samples as characterized in Section 3.3.2.

3.2.3 Effect of nozzle tilt angle

As discussed above, increasing the nozzle tilt angle will help achieve a smoother, more natural flow of coextruded carbon fibers and PLA melt, which was shown to improve printability window in Fig. 5 with higher maximum print speeds achieved. The effect of nozzle tilt angle on obtained

mechanical properties is also studied for CFRC samples printed under a constant print speed of 800 mm/min and a material deposition rate of 5.7 g/min, and the results are summarized in Fig. 8. The parameters for this study were chosen since they corresponded to the lowest mechanical properties observed in Section 3.2.1 despite having a relatively higher fiber volume fraction than most other samples. This parameter set was near the boundary where fiber exposure and tangling were found to begin, and the low mechanical properties of samples printed with these parameters, and a nozzle inclination angle of 0°, could be partially attributed to the scratching effect causing a degree fiber breakage during printing. It was hypothesized that fiber scratching and breakage may be alleviated by increasing the nozzle tilt angle, hence improving flexural strength and modulus of samples. All tested samples exhibited acceptable print quality with no fiber tangling/exposure. Both flexural strength and modulus first increased as the

Fig. 7 Flexural strength and modulus measured through four-point bending tests for PLA samples and continuous CFRC samples printed at a material deposition rate of 5.7 g/min and a nozzle tilt angle of 0° with varying print speeds



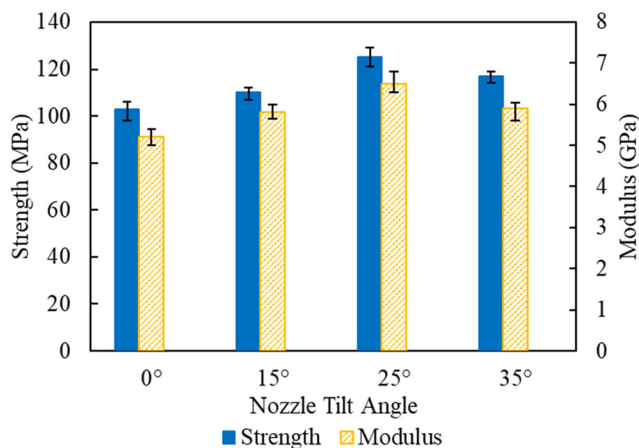


Fig. 8 Measured flexural strength and modulus through four-point bending tests of continuous CFRC samples with varying nozzle tilt angles. A constant print speed of 800 mm/min and a material deposition rate of 5.7 g/min were used

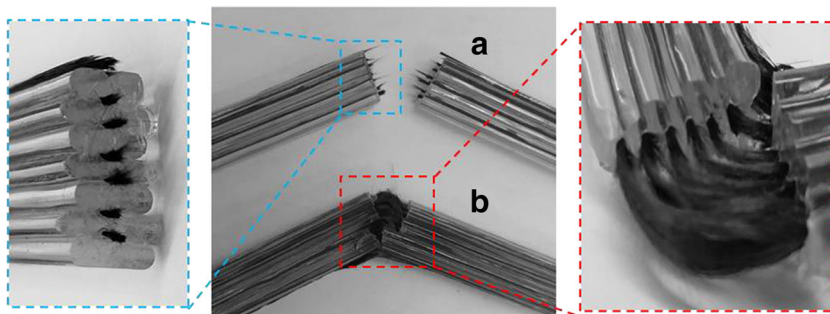
nozzle tilt angle increased. Compared to those measured at a nozzle tilt angle of 0°, a maximum 21% improvement in average flexural strength and a maximum 25% improvement in average flexural modulus were achieved at a nozzle tilt angle of 25°. Further increasing the nozzle tilt angle to 35° lowered the obtained mechanical strength and modulus. The variations observed in mechanical properties are expected to be affected by fiber breakage and void formation during the printing process, which were further studied through microstructure analysis in Section 3.3.3.

3.3 Microstructure characterization

3.3.1 Effect of material deposition rate

Figure 9 shows the fracture surfaces of two typical CFRC samples obtained at a print speed of 800 mm/min with two different deposition rates (i.e., 5.7 g/min and 13.3 g/min). Different damage mechanisms were obviously observed for the samples printed at the different material deposition rates. The fracture pattern of the sample obtained at the deposition rate of 5.7 g/min was dominated by PLA matrix cracking with severe fiber pull-outs observed. This is believed to be attributed to poor fiber-matrix bonding. In contrast, for the sample

Fig. 9 Fracture surfaces of typical continuous CFRC samples obtained from four-point bending tests, showing different fracture mechanisms for the samples at a print speed of 800 mm/min with two different deposition rates: (a) 13.3 g/min and (b) 5.7 g/min

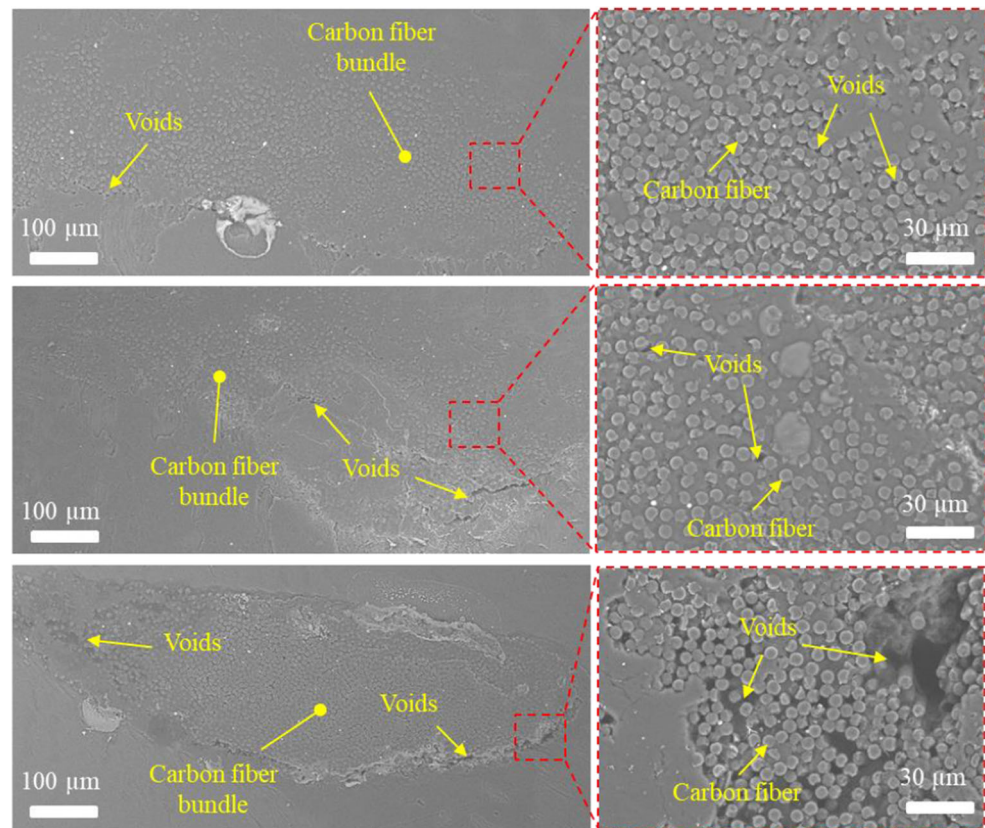


printed at the higher deposition rate of 13.3 g/min, the damage mechanism was governed by simultaneous fiber breakage and PLA matrix cracking, indicating good bonding between the fibers and the matrix material. The stronger fiber-matrix bonding achieved at higher deposition rates more effectively reinforces the CFRC samples, thus yielding higher mechanical properties compared to those obtained at lower material deposition rates (see Fig. 6).

The different fiber-matrix bonding is believed to be due to different fiber wetting conditions obtained at different deposition rates. The transverse cross sections of the CFRC samples at different deposition rates are further compared in Fig. 10. Two types of voids are typically observed, i.e., voids around carbon fiber bundle and voids around/between single carbon fiber filaments as shown in the close-up views in Fig. 10. For the CFRC sample printed at the deposition rates of 5.7 g/min and 7.4 g/min, obvious voids are observed around the carbon fiber bundle in Fig. 10a and b. In contrast, for the higher deposition rate of 13.3 g/min, a better wetting condition is observed with no obvious voids observed between the fiber bundle and the PLA matrix material in Fig. 10c. The measured void fraction of the CFRC samples is summarized in Fig. 11. The void fraction decreased as the material deposition rate increased with the void fraction obtained at the deposition rate of 5.7 g/min over 2.5-fold of that found at 13.3 g/min. These void defects will weaken the fiber-matrix bonding and lower the obtained mechanical properties.

A higher material deposition rate is believed to be accompanied by a higher PLA melt flow rate. The overall improved flowability increases polymer chain movement at molecular level that in turn results in localized increased in plasticity and decreased in glass transition temperature [39, 40]. Permeability of such polymers is dictated by their resulting softer polymer chains [41], thus promoting wetting between the PLA melt and the carbon fibers within the printed CFRC samples. These processes combined to achieve improved fiber-matrix bonding, thus leading to better mechanical properties at higher deposition rates. It should be noted that despite lower fiber volume fraction at higher deposition rates [11], our microstructural analysis indicated that fiber impregnation by the matrix, and the corresponding void formation, was the dominant mechanism controlling mechanical properties.

Fig. 10 Microscopic images of the transverse cross sections of continuous CFRC samples at a print speed of 800 mm/min and a nozzle tilt angle of 0° at different deposition rates: (a) 5.7 g/min, (b) 7.4 g/min, and (c) 13.3 g/min



When the material deposition rate was high, the increased PLA melt flow rate provided better penetration into the carbon fiber network and thereby improving fiber wetting and reducing voids.

3.3.2 Effect of print speed

The transverse cross sections of the CFRC samples obtained at different print speeds are also compared in Fig. 12. As the print speed increased from 400 to 1000 mm/min, more obvious voids around carbon fiber bundle were observed. The

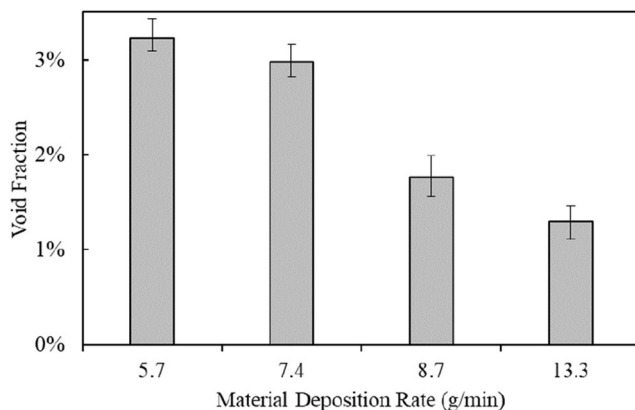


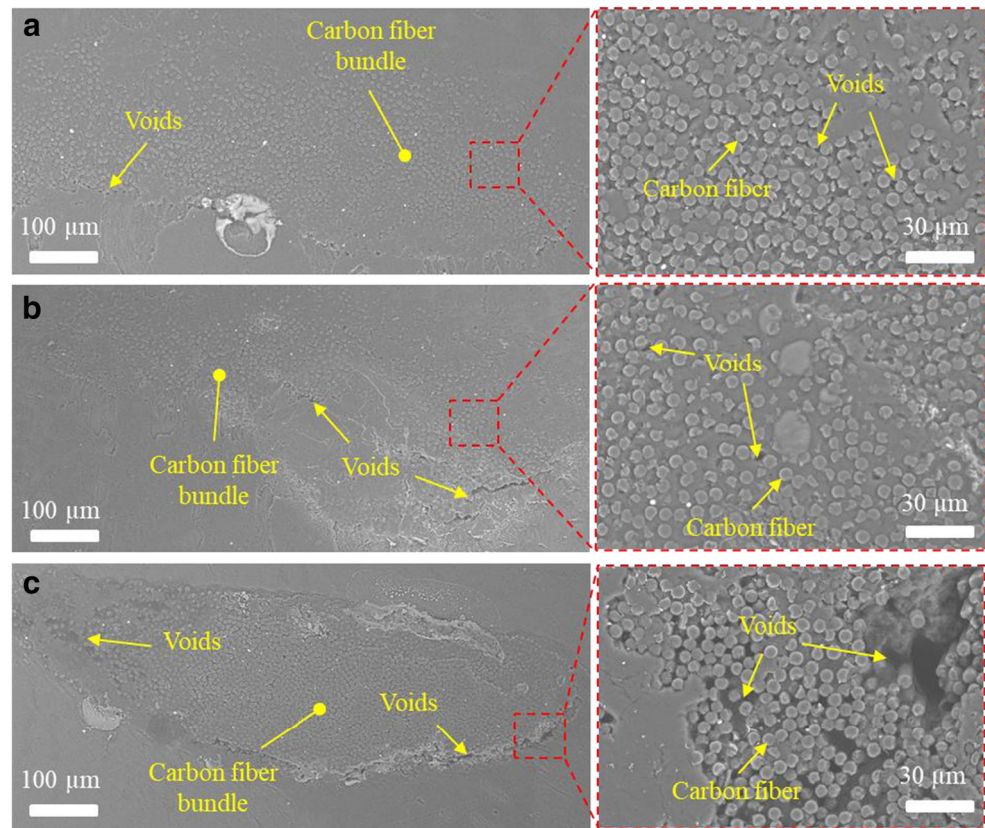
Fig. 11 Measured void fraction within printed continuous CFRC samples at a print speed of 800 mm/min and a nozzle tilt angle of 0° with varying material deposition rates

corresponding measured void fraction in Fig. 13 also increases to 4.0% at the print speed of 1000 mm/min, nearly four times of that at the print speed of 400 mm/min. Due to the higher amount of voids observed as the print speed increases, the residual voids within the CFRC samples in Fig. 12 will work crack nucleation sites and further weaken obtained mechanical properties. It explains the decreasing flexural strength and modulus observed in Fig. 7 after increasing the print speed from 400 to 1000 mm/min despite higher fiber volume fraction [11]. The void fraction is believed to be affected by fiber impregnation time during the printing process. A higher print speed decreased the fiber impregnation time, leading to worse wetting and more residual voids as well as poorer interfacial bonding between carbon fibers and PLA matrix material. To achieve high-speed 3D printing process, it will thus be necessary to compensate the reduced fiber impregnation time at increased print speed through controlling printing conditions so that a good fiber wetting condition can still be obtained.

3.3.3 Effect of nozzle tilt angle

Microscopic images of the cross sections of printed CFRC samples with different nozzle tilt angles were further investigated. The morphology of reinforcing continuous carbon fibers is first examined in Fig. 14. Although no fiber tangling or exposure was observed for the selected printing parameters

Fig. 12 Microscopic images of the transverse cross sections of continuous CFRC samples printed with a material deposition rate of 5.7 g/min and a nozzle tilt angle of 0° at different print speeds: (a) 400 mm/min, (b) 600 mm/min, and (c) 1000 mm/min



(within the printability window), more obvious fiber breakage was found when a smaller nozzle tilt angle was used, indicating that scratching by the extrusion nozzle due to drawing force also caused fiber damage. Intact fiber bundle was obtained after increasing the tilt angle above 25°. This helps explain the relatively higher mechanical properties in Fig. 8 found for the CFRC samples printed at the nozzle tilt angle of 25°.

On the other hand, an increased amount of voids is observed from the transverse cross sections of the printed CFRC samples in Fig. 15 as the nozzle tilt angle increased.

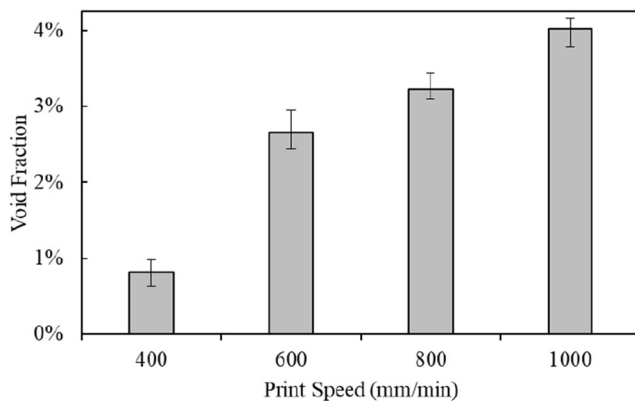


Fig. 13 Measured void fraction within printed continuous CFRC samples at a material deposition rate of 5.7 g/min and a nozzle tilt angle of 0° with varying print speeds

The void fraction is further measured as summarized in Fig. 16. Nearly 7.1% void fraction was observed for the samples printed at the nozzle tilt angle of 35°, increased from 3.2% at the nozzle tilt angle of 0°. It explains the lowered flexural strength and modulus observed in Fig. 8 after increasing the nozzle tilt angle from 25° to 35°. The results indicated that although increasing nozzle tilt angle enabled a more natural flow of extrudate, the improved fiber reinforcement (e.g., fewer fiber tangling/exposure/breakage) was offset by increased void formation. Hence, the optimal nozzle tilt angle existed at 25° for the printing conditions used in this study. The increased void fraction is believed to be caused by decreased pressure applied on the extrudate when a higher tilt angle was used. While future studies will be performed to measure and control pressure applied on extrudates during the 3D printing process, the decreased pressure caused by nozzle tilt angle may be compensated by increasing layer thickness or material deposition rate to achieve optimal printing conditions.

3.4 Fiber impregnation process

The fiber wetting conditions discussed above are believed to be affected by fiber impregnation process as illustrated in Fig. 17. During the printing process, the fiber bundle and the PLA melt are coextruded and then deposited on the substrate. In the meantime, the PLA melt flows into the continuous fiber

Fig. 14 Microscopic images of the longitudinal cross sections of continuous CFRC samples printed with different nozzle tilt angles of (a) 0°, (b) 15°, (c) 25°, and (d) 35°. A constant print speed of 800 mm/min and a material deposition rate of 5.7 g/min were used

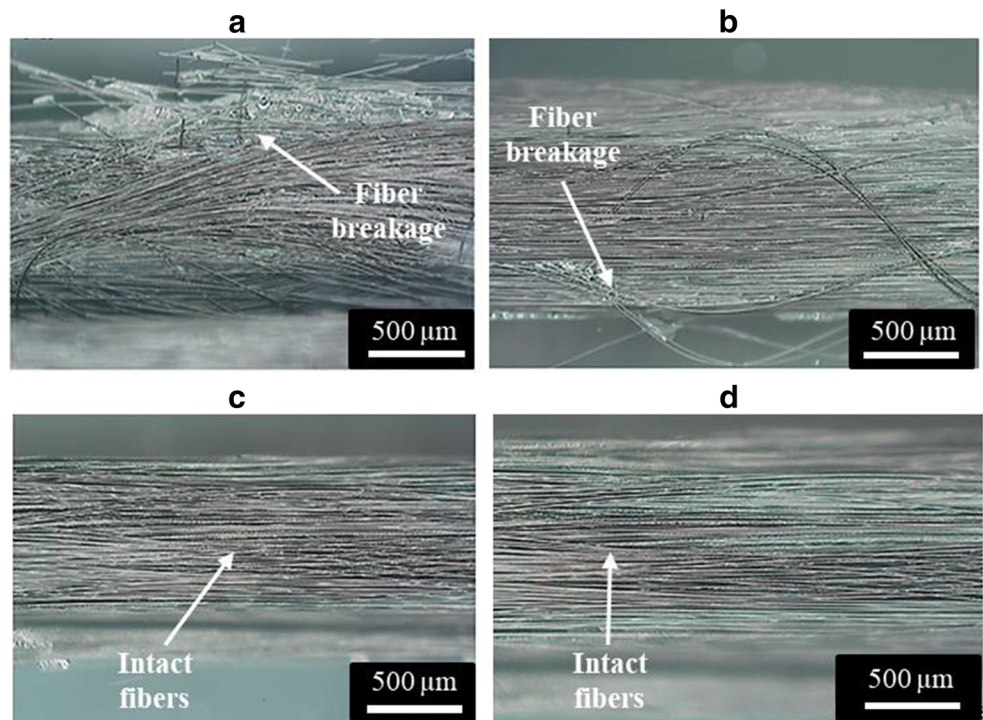
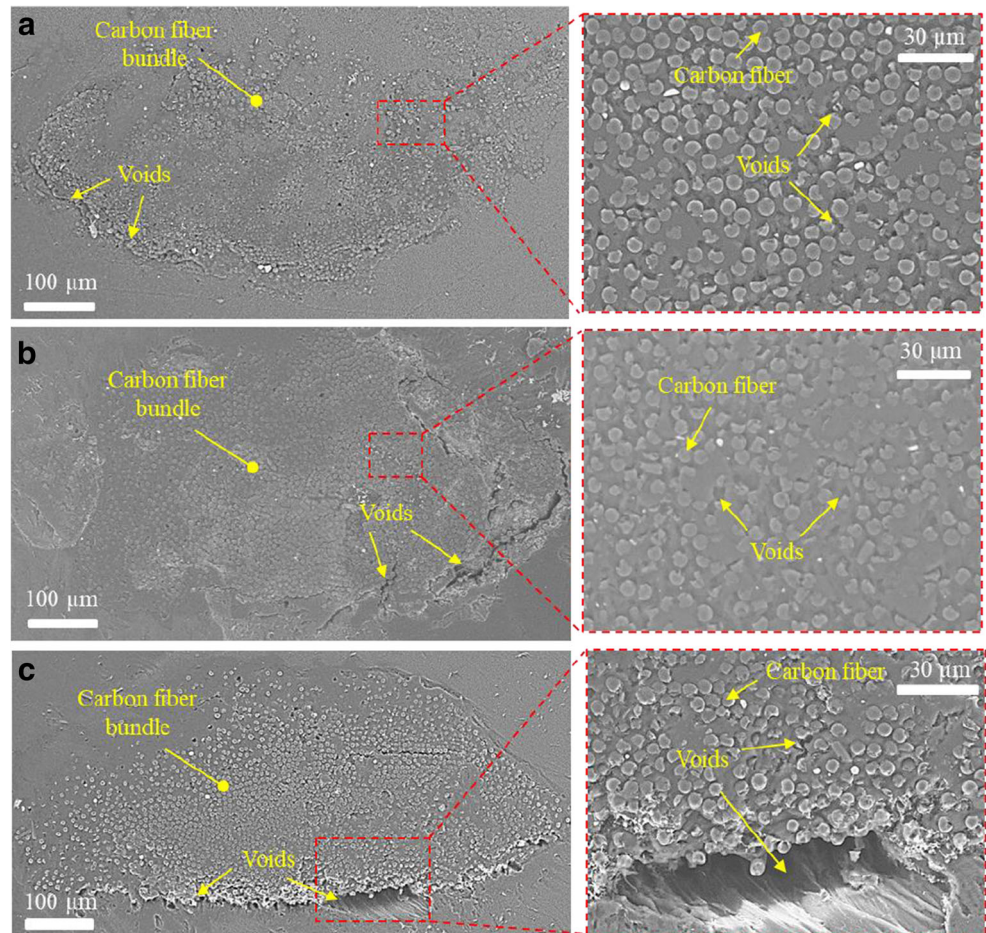


Fig. 15 Microscopic images of the transverse cross sections of continuous CFRC samples printed with different nozzle tilt angles of (a) 15°, (b) 25°, and (c) 35°. A constant print speed of 800 mm/min and a material deposition rate of 5.7 g/min were used



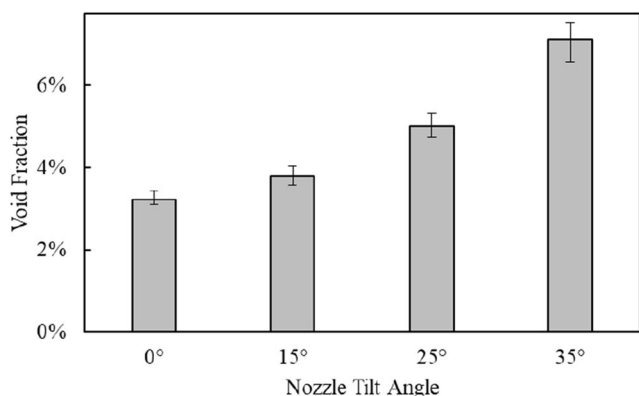


Fig. 16 Measured void fraction within printed CFRC samples in terms of nozzle tilt angle. A constant print speed of 800 mm/min and a material deposition rate of 5.7 g/min were used

bundle under pressure. It is believed that the fiber impregnation mechanisms during the printing process in this study is governed by combined PLA melt penetration of carbon fiber network at the meso-scale and single fiber wetting process at the micro-scale.

The transverse cross section of carbon fiber bundle in Fig. 17a is shown in Fig. 17b–d at the meso-scale. The melt flow will penetrate through the carbon fiber network under pressure [42]. The impregnation at this stage is believed to be determined by melt flow rate. If a higher material deposition rate is utilized, the corresponding increased PLA melt flow rate makes it faster for the PLA melt to penetrate the carbon fiber network within limited impregnation time at a constant print speed. A higher deposition rate achieved by a higher extruder rotation speed in this study is also expected to be associated with higher melt flow pressure, making the PLA melt to more easily penetrate the carbon fiber network. These processes are believed to be associated with the improved fiber wetting conditions observed above after the material deposition rate

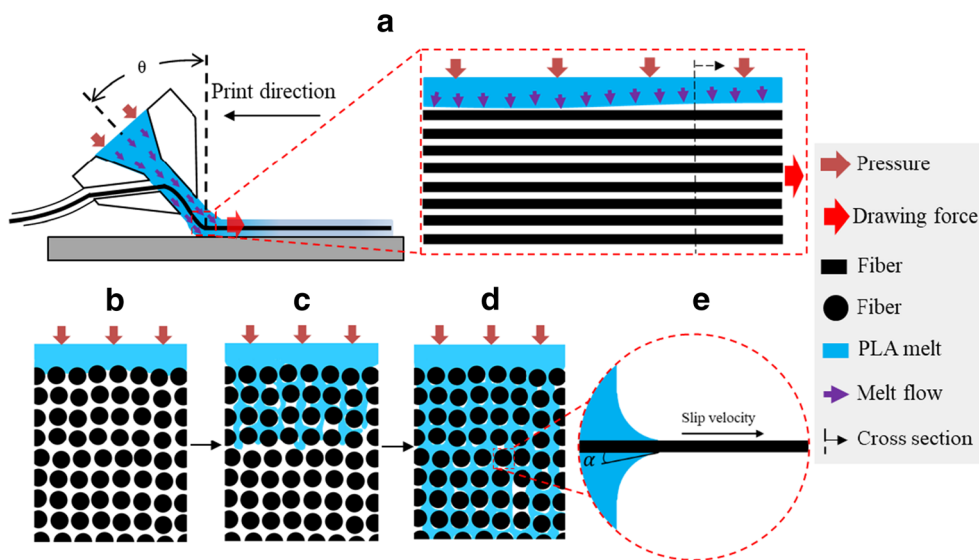
increased. However, an increased nozzle tilt angle for the proposed multi-axis 3D printing process in this study is believed to lower the melt flow pressure, making the PLA melt harder to penetrate the carbon fiber network and yielding poorer fiber wetting conditions observed in Fig. 15. On the other hand, if a higher print speed is implemented, the total amount of fiber impregnation time will be decreased, limiting the degree of impregnation that can be achieved at a given melt flow rate (i.e., a constant material deposition rate). This will thus yield poorer fiber wetting conditions, possibly still at the stage shown in Fig. 17c, with relatively higher amount of residual voids around carbon fiber bundle observed above (i.e., at the print speed of 1000 mm/min in Figs. 12C and 13).

With sufficient PLA melt flow around carbon fibers in Fig. 17d, fiber-PLA adhesion will then be determined by the single fiber wetting process at the micro-scale as shown in Fig. 17e. For a given polymer composition, e.g., PLA in this study, the wettability of a single carbon fiber at the micro-scale is affected by slip velocity [43] between moving fibers and melt flow in Fig. 17a and is typically characterized by a dynamic contact angle (α) on the fiber surface as shown in Fig. 17e. With a sufficiently long impregnation time (e.g., low print speed) and a high melt flow rate (e.g., high material deposition rate), the degree of impregnation within the printed CFRC samples in Fig. 17d will then be mainly affected by the single fiber wetting properties as represented by the dynamic contact angle (α), which may create nucleation sites for residual voids around/between single carbon fiber filaments typically observed in the close-up views of CFRC microstructure above.

3.5 Demonstration of AM of CFRC structures

Printing of CFRC parts using the proposed AM method is demonstrated with the obtained samples shown in Fig. 18.

Fig. 17 a shows schematics of fiber impregnation process; b–d show the transverse cross-sections of carbon fiber bundle and impregnation mechanisms as combined PLA penetration of carbon fiber network at the meso-scale and single fiber wetting process at the micro-scale in e



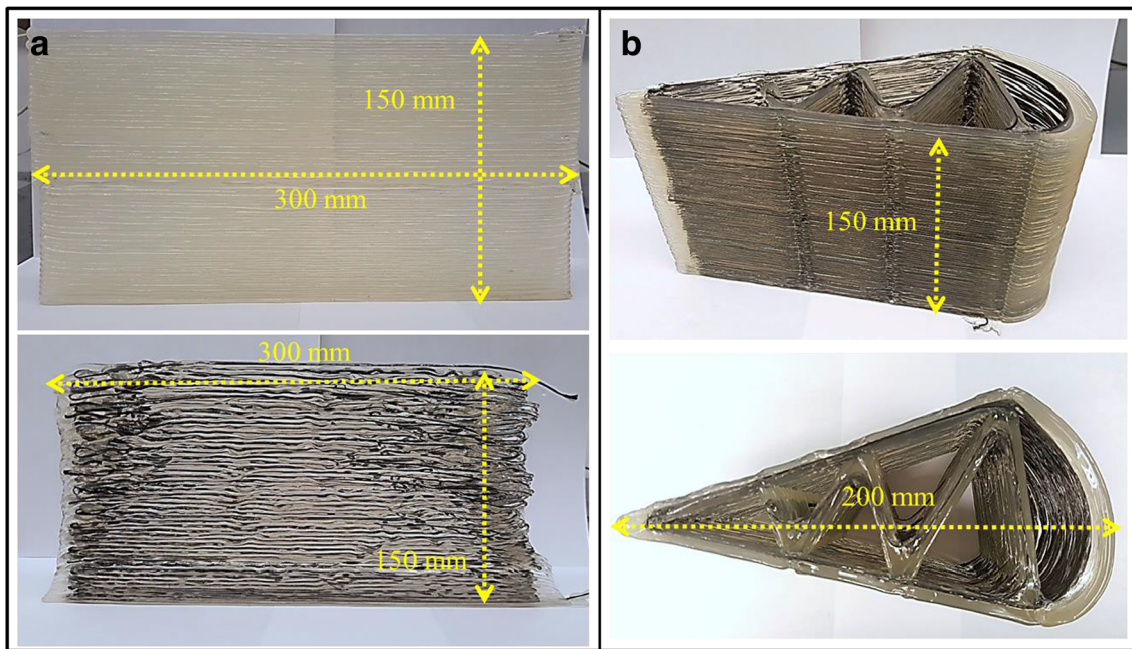


Fig. 18 CFRC samples printed by the AM setup with continuous carbon fibers at the print speed of 800 mm/min, deposition rate of 13.3 g/min, and nozzle tilt angle of 0°. **a** shows thin-wall structures printed without

(top) and with (bottom) continuous carbon fiber reinforcement, and **b** shows a wing-rib structure printed with a single continuous carbon fiber bundle as reinforcement

Thin-wall samples reinforced with and without carbon fibers are first printed for comparison in Fig. 18a. A print speed of 800 mm/min and a deposition rate of 13.3 g/min were used, with a nozzle tilt angle of 0°. It is worth noting that each CFRC sample was printed with a single continuous carbon fiber bundle shown as the dark phase within the parts. A complex geometry CFRC structure printed at the selected conditions is further demonstrated in Fig. 18b. All the samples shown in Fig. 18 are completed within 2 h, attributed to the relatively high deposition rate of 13.3 g/min employed. Note that these large parts normally would take days to print using a typical FFF process (e.g., with material deposition rates varying between 0.17 g/min and 0.46 g/min [11]).

4 Conclusions

In this study, a parametric study was performed experimentally to investigate the effects of several factors, including material deposition rate, print (nozzle traverse) speed, and nozzle tilt angle, that affect high-speed 3D printing of continuous CFRC samples. Specifically, a novel multi-axis 3D printing approach was utilized to maintain a constant nozzle tilt angle following a print toolpath. Without multi-axis 3D printing, increasing print speed increased fiber tangling and exposure, and lower mechanical properties were measured due to decreased fiber impregnation time and poorer fiber-matrix bonding. On the other hand, increasing material deposition rate and nozzle tilt

angle enabled the implementation of higher print speeds, thus higher AM productivity, without sacrificing print quality. It is believed that increased flowability due to improved melt flow rate and pressure at higher material deposition rate improve fiber impregnation quality. Increasing nozzle tilt angle achieved a smoother, more natural flow of extrudate and lowered fiber breakage, thus yielding improved CFRC mechanical properties. However, void formation increased in the meantime due to decreased pressure applied on extrudate. The void formation is believed to be governed by combined melt penetration of carbon fiber network at the meso-scale and single fiber wetting process at the micro-scale, as affected by melt flow rate, pressure, and impregnation time as well as single fiber wettability. It also helped explain the two types of voids typically observed within the printed CFRC microstructure, i.e., voids around carbon fiber bundle and voids around/between single carbon fiber filaments. The understanding of the 3D printing processes of continuous CFRCs in this study will further help obtain optimal printing conditions for design and fabrication of large-volume continuous CFRC structural components via high-speed 3D printing.

Authors' contributions Conceptualization, J.M.P. and X.D.; methodology, J.M.P., A.R.T., and X.D.; investigation, J.M.P., A.R.T., and X.D.; writing—original draft preparation, J.M.P., A.R.T., and X.D.; writing—review and editing, X.D. and M.C.L.; supervision, X.D. and M.C.L.; project administration, X.D. and M.C.L.; funding acquisition, X.D. and M.C.L.

Funding The authors acknowledge the funding support by Automated Precision Inc. and the Intelligent Systems Center at the Missouri University of Science and Technology for the research work presented in this paper.

Data availability The data that support the findings of this study are available from the corresponding author, X.D., upon reasonable request.

Declarations

Ethical approval Not applicable

Consent to participate Not applicable

Consent to publish Not applicable

Conflict of interests The authors declare that they have no conflict of interest.

References

- Goh GD, Agarwala S, Goh GL, Dikshit V, Sing SL, Yeong WY (2017) Additive manufacturing in unmanned aerial vehicles (UAVs): challenges and potential. *Aerosp Sci Technol* 63:140–151
- Matsuzaki R, Ueda M, Namiki M, Jeong TK, Asahara H, Horiguchi K, Nakamura T, Todoroki A, Hirano Y (2016) Three-dimensional printing of continuous-fiber composites by in-nozzle impregnation. *Sci Rep* 6:23058
- Ning F, Cong W, Hu Y, Wang H (2017) Additive manufacturing of carbon fiber-reinforced plastic composites using fused deposition modeling: effects of process parameters on tensile properties. *J Compos Mater* 51(4):451–462
- Dudek P (2013) FDM 3D printing technology in manufacturing composite elements. *Arch Metall Mater* 58(4):1415–1418
- Farahani RD, Dalir H, Le Borgne V, Gautier LA, El Khakani MA, Lévesque M, Theriault D (2012) Direct-write fabrication of free-standing nanocomposite strain sensors. *Nanotechnology* 23(8):085502
- Ferreira RTL, Amatte IC, Dutra TA, Bürger D (2017) Experimental characterization and micrography of 3D printed PLA and PLA reinforced with short carbon fibers. *Compos Part B Eng* 124:88–100
- Papon EA, Haque A (2019) Fracture toughness of additively manufactured carbon fiber reinforced composites. *Addit Manuf* 26:41–52
- Justo J, Távora L, García-Guzmán L, París F (2018) Characterization of 3D printed long fibre reinforced composites. *Compos Struct* 185:537–548
- Li N, Li Y, Liu S (2016) Rapid prototyping of continuous carbon fiber reinforced polylactic acid composites by 3D printing. *J Mater Process Technol* 238:218–225
- Yao X, Luan C, Zhang D, Lan L, Fu J (2017) Evaluation of carbon fiber-embedded 3D printed structures for strengthening and structural-health monitoring. *Mater Des* 114:424–432
- Tian X, Liu T, Yang C, Wang Q, Li D (2016) Interface and performance of 3D printed continuous carbon fiber reinforced pla composites. *Compos A: Appl Sci Manuf* 88:198–205
- Zhang M, Zhao M, Jian M, Wang C, Yu A, Yin Z, Liang X, Wang H, Xia K, Liang X, Zhai J, Zhang Y (2019) Printable smart pattern for multifunctional energy-management e-textile. *Matter* 1(1):168–179
- Kabir SMF, Mathur K, Seyam AFM (2020) A critical review on 3D printed continuous fiber-reinforced composites: history, mechanism, materials and properties. *Compos Struct* 232:111476
- Moreno Nieto D, Casal López V, Molina SI (2018) Large-format polymeric pellet-based additive manufacturing for the naval industry. *Addit Manuf* 23:79–85
- Ye W, Lin G, Wu W, Geng P, Hu X, Gao Z, Zhao J (2019) Separated 3D printing of continuous carbon fiber reinforced thermoplastic polyimide. *Compos A Appl Sci Manuf* 121:457–464
- Duty CE, Kunc V, Compton B, Post B, Erdman D, Smith R, Lind R, Lloyd P, Love L, E., D. C. (2017) Structure and mechanical behavior of big area additive manufacturing (BAAM) materials. *Rapid Prototyp J* 23(1):181–189
- Rakhshbahar M, Sinapius M (2018) A novel approach: combination of automated fiber placement (AFP) and additive layer manufacturing (ALM). *J Compos Sci* 2(3):42
- Degenhardt R, Castro SGP, Blachut J, Arbelo MA, Khakimova R (2017) Stability of composite shell-type structures. In: *Stability and vibrations of thin-walled composite structures*, edited by Abramovich H. Elsevier, pp 253–428
- Cincinnati Incorporated (2020) Big area additive manufacturing 3D printer [Online]. Available: <https://www.e-ci.com/baam>. [Accessed: 13-Sep-2020].
- Woern AL, Byard DJ, Oakley RB, Fiedler MJ, Snabes SL, Pearce JM (2018) Fused particle fabrication 3-D printing: recycled materials' optimization and mechanical properties. *Materials (Basel)* 11(8):1413
- Cead BV (2019) CFAM Prime. CEAD Addit Manuf [Online]. Available: <https://cead-am.com/>. [Accessed: 13-Sep-2020].
- Liu T, Tian X, Zhang Y, Cao Y, Li D (2020) High-pressure interfacial impregnation by micro-screw in-situ extrusion for 3D printed continuous carbon fiber reinforced nylon composites. *Compos A: Appl Sci Manuf* 130:105770
- Zhang H, Liu D, Huang T, Hu Q, Lammer H (2020) Three-dimensional printing of continuous flax fiber-reinforced thermoplastic composites by five-axis machine. *Materials (Basel)* 13:1678
- Bhatt PM, Malhan RK, Shembekar AV, Yoon YJ, Gupta SK (2020) Expanding capabilities of additive manufacturing through use of robotics technologies: a survey. *Addit Manuf* 31:100933
- Pan Y, Zhou C, Chen Y, Partanen J (2014) Multitool and multi-axis computer numerically controlled accumulation for fabricating conformational features on curved surfaces. *J Manuf Sci Eng Trans ASME* 136(3):031007
- Quan Z, Larimore Z, Wu A, Yu J, Qin X, Mirotznik M, Suhr J, Byun JH, Oh Y, Chou TW (2016) Microstructural design and additive manufacturing and characterization of 3D orthogonal short carbon fiber/acrylonitrile-butadiene-styrene preform and composite. *Compos Sci Technol* 126:139–148
- Ishak I, Laroche P (2016) Robot arm platform for additive manufacturing: 3D lattice structures. In: *30th Florida Conference on Recent Advances in Robotics May 11-12, 2017, Boca Raton, Florida, USA*
- Yerazunis WS, Barnwell III JC, Nikovski DN (2016) Strengthening ABS, nylon, and polyester 3D printed parts by stress tensor aligned deposition paths and five-axis printing. In: *Proceedings of the Solid Freeform Fabrication Symposium, 2016, 1259–1271, Austin, Texas, USA*
- Alsharhan AT, Centea T, Gupta SK (2017) Enhancing mechanical properties of thin-walled structures using non-planar extrusion based additive manufacturing. In: *ASME 12th International Manufacturing Science and Engineering Conference collocated with the JSME/ASME 2017 6th International Conference on Materials and Processing, 2017, Los Angeles, California, USA*
- Sinkez PG, De Backer W (2019) Design for multi-axis fused filament fabrication with continuous fiber reinforcement: unmanned

- aerial vehicle applications. In: AIAA Scitech 2019 Forum, AIAA 2019-0156, 2019, San Diego, California, USA
31. Pérez-Pacheco E, Cauich-Cupul JI, Valadez-González A, Herrera-Franco PJ (2013) Effect of moisture absorption on the mechanical behavior of carbon fiber/epoxy matrix composites. *J Mater Sci* 48(5):1873–1882
 32. Liu X, Chi B, Jiao Z, Tan J, Liu F, Yang W (2017) A large-scale double-stage-screw 3D printer for fused deposition of plastic pellets. *J Appl Polym Sci* 134(31):45147
 33. Tian X, Liu T, Wang Q, Dilmurat A, Li D, Ziegmann G (2017) Recycling and remanufacturing of 3D printed continuous carbon fiber reinforced PLA composites. *J Clean Prod* 142:1609–1618
 34. Mehndiratta A, Bandyopadhyaya S, Kumar V, Kumar D (2018) Experimental investigation of span length for flexural test of fiber reinforced polymer composite laminates. *J Mater Res Technol* 7(1): 89–95
 35. Chen R, Misra M, Mohanty AK (2013) Injection-moulded biocomposites from polylactic acid (PLA) and recycled carbon fibre: evaluation of mechanical and thermal properties. *J Thermoplast Compos Mater* 27(9):1286–1300
 36. Bettini P, Alitta G, Sala G, Di Landro L (2017) Fused deposition technique for continuous fiber reinforced thermoplastic. *J Mater Eng Perform* 26(2):843–848
 37. Han X, Yang D, Yang C, Spintzyk S, Scheideler L, Li P, Li D, Geis-Gerstorf J, Rupp F (2019) Carbon fiber reinforced PEEK composites based on 3D-printing technology for orthopedic and dental applications. *J Clin Med* 8(2):240
 38. Schindelin J, Arganda-Carreras I, Frise E, Kaynig V, Longair M, Pietzsch T, Preibisch S, Rueden C, Saalfeld S, Schmid B, Tinevez J-Y, White DJ, Hartenstein V, Eliceiri K, Tomancak P, Cardona A (2012) Fiji: an open-source platform for biological-image analysis. *Nat Methods* 9(7):676–682
 39. Peppas NA, Wu JC, von Meerwall ED (1994) Mathematical modeling and experimental characterization of polymer dissolution. *Macromolecules* 27(20):5626–5638
 40. Wallow TI, Morales AM, Simmons BA, Hunter MC, Krafcik KL, Domeier LA, Sickafoose SM, Patel KD, Gardea A (2007) Low-distortion, high-strength bonding of thermoplastic microfluidic devices employing case-II diffusion-mediated permeant activation. *Lab Chip* 7(12):1825–1831
 41. Hohimer C, Christ J, Aliheidari N, Mo C, Ameli A (2017) 3D printed thermoplastic polyurethane with isotropic material properties. In: *Behavior and Mechanics of Multifunctional Materials and Composites 2017*. SPIE, Portland, p 1016511
 42. Ngo SI, Lim Y-I, Hahn M-H, Jung J (2018) Prediction of degree of impregnation in thermoplastic unidirectional carbon fiber Prepreg by multi-scale computational fluid dynamics. *Chem Eng Sci* 185: 64–75
 43. Qiu S, Fuentes CA, Zhang D, Van Vuure AW, Seveno D (2016) Wettability of a single carbon fiber. *Langmuir* 32(38):9697–9705

Publisher's note Springer Nature remains neutral with regard to jurisdictional claims in published maps and institutional affiliations.